

Thermodynamics of network model fitting with spectral entropies

Carlo Nicolini,^{1,2} Vladimir Vlasov,^{1,2} and Angelo Bifone¹

¹*Center for Neuroscience and Cognitive Systems, Istituto Italiano di Tecnologia, Corso Bettini 31, 38068 Rovereto (TN), Italy*

²*These authors contributed equally to this work*

(Dated: May 9, 2022)

An information theoretic approach inspired by quantum statistical mechanics was recently proposed as a means to optimize network models and to assess their likelihood against synthetic and real-world networks. Importantly, this method does not rely on specific topological features or network descriptors, but leverages entropy-based measures of network distance. Entertaining the analogy with thermodynamics, we provide a physical interpretation of model hyperparameters and propose analytical procedures for their estimate. These results enable the practical application of this novel and powerful framework to network model inference. We demonstrate this method in synthetic networks endowed with a modular structure, and in real-world brain connectivity networks.

I. INTRODUCTION

Many natural and artificial phenomena can be represented as networks of interacting elements. The mathematical framework of network theory can be applied across disciplines, ranging from sociology to neuroscience, and provides a powerful means to investigate a variety of diverse phenomena [1]. Unveiling the structural and organizational principles of complex networks often implies comparison with statistical network models. Generative models, for example, describe mechanisms of network wiring and evolution [2, 3], or the constraints that may have contributed to shaping the network topology during its development [4]. Null models are used to describe maximally random networks with specific features, for example prescribed sequences of node degrees [5].

Maximum likelihood approaches have been proposed to compare the ability of different models to describe real-world networks and to optimize model parameters to best fit experimental networks. However, application of these methods to model inference presents drawbacks, as they do not take into account the entire network structure but only focus on specific features or constraints [6].

Recently, an information theoretic framework inspired by quantum statistical mechanics principles has been proposed as a tool to assess and optimize network models [7]. This approach relies on the minimization of the relative entropy based on the network spectral properties. Importantly, relative entropy does not depend on a distribution of specific descriptors, but considers the network as a whole. However, this representation introduces an external, tunable hyperparameter β ; the optimal estimate from the relative entropy minimization procedure critically depends on the choice of β , a major limitation to the practical use of this framework.

Relative entropy is a central concept in thermodynamics of information (see review [8]) and is defined on the

basis of the density matrix. In light of this thermodynamic analogy, here we build a physical interpretation of this approach to network optimization and fitting, where β plays the role of an inverse temperature. This provides criteria for a rigorous selection of the optimal β , and enables the practical application of relative entropy minimization in the optimal reconstruction of parameters for different network models.

The paper is structured as follows. First, we present theoretical framework of maximum entropy null models as a way to generate maximally random ensemble of networks with given constraints. We move on to discussing how the Erdős-Rényi random graph and the configuration model emerge naturally from these ideas.

In the second section we shift to thermodynamic realm, presenting the von Neumann entropy of complex networks and the idea of relative entropy as a tool for network comparison. We discuss a thermodynamic interpretation of the relative entropy between empirical and model networks and provide a concise closed form expression for its gradients with respect to the model parameters. This permits continuous optimization methods, which are dependent on the inverse temperature hyper-parameter. We calculate analytically the optimal temperature parameter of an Erdős-Rényi or planted partition models. Furthermore, we generalize this result to more complex models with the help of numerical simulations.

Importantly, we show the advantages of the spectral entropy approach with respect to other maximum likelihood methods. Finally, we demonstrate the use of spectral entropies for the optimization of a generative model of neural connectivity in a real-world dataset.

II. MODELS OF COMPLEX NETWORKS

We summarize here a few definitions which are necessary to make this paper self-contained. Let us consider here simple binary undirected graphs $G = (V, E)$ with $|V| = n$ number of nodes and $|E| = m$ number of links.

The adjacency matrix is denoted as $\mathbf{A} = \{a_{ij}\}$ and the (combinatorial) graph Laplacian as $\mathbf{L} = \mathbf{D} - \mathbf{A}$, where \mathbf{D} is the diagonal matrix of the node degrees. Notably, the (combinatorial) Laplacian matrix associated with an undirected graph is a positive definite matrix, meaning that all its eigenvalues $\lambda_1 \geq \dots \geq \lambda_n = 0$ are positive and real. A random graph model is an ensemble of networks randomly distributed around some specific network property, with a probability distribution $\mathcal{P}(\Omega)$. For example, in the Gilbert random graph model the probability distribution $\mathcal{P}(G)$ is sharply peaked in $\mathcal{P}(G) = 1/\Omega$ for graphs with n nodes and exactly m edges, and is zero otherwise [1]. This distribution is well described in statistical mechanics as the *microcanonical* ensemble, as it enforces the constraints strictly.

However, given the combinatorial complexity of dealing with the micro-canonical description, it is easier to fix the average value of observables of interest rather than working with exact constraints. This approach gives rise to the canonical ensemble of random graphs [1, 9]. This type of models has the same role in the study of complex networks as the Boltzmann distribution in classical statistical mechanics; it gives the maximally uninformed prediction of some network properties subject to the imposed constraints.

These ideas can be dated back to the Jaynes' maximum entropy principle [10]. In this sense, the maximally random ensemble of graphs satisfying the imposed topological constraints on average also takes the name of the Exponential Random Graph Model (ERGM) in the social sciences [1, 5]. In the settings of the ERGM one can define a graph on n nodes as the result of a random process where each edge (i, j) is sampled with a probability $p_{ij}(\theta)$ described with a vector of parameters θ . In its simplest implementation, the ERGM results in the Erdős-Rényi [11] model, where the link probability is constant.

On the other hand, if one wants to generate the maximally random network that maintains the desired degree sequence $\{k_i\}$, the resulting ensemble is called the Undirected Binary Configuration Model (UBCM) [9, 12, 13]. Being the degree an entirely local topological property, it is affected by the intrinsic properties of vertices. For this reason, one can assign a hidden variable $x_i \geq 0$ to each node. Its value acts as a fitness score, which is hypothesized to be proportional to the expected node degree [12]. If two nodes have a high fitness score, they are more

likely to be connected by a link. In this model one can describe the link probability as the normalized product of their scores [9, 13, 14], resulting in the following expected link probability:

$$p_{ij} = \langle a_{ij} \rangle = \frac{x_i x_j}{1 + x_i x_j} \quad (1)$$

The values of x_i are obtained by numerical optimization of a specifically designed likelihood function [13, 15]. In this framework, the hidden variables x_i are the Lagrange multipliers of the constrained problem that ensures the expected degree $\langle k_i \rangle = \sum_{j \neq i} \langle a_{ij} \rangle$ of the vertex i equals on average its empirical value k_i . Interestingly this model highlights the *fermionic* properties of the links, as they are modeled like particles with only two states, namely the link being present or not.

If the network is sufficiently random, the degree-sequence alone can model the higher order patterns like the clustering coefficient or the average nearest neighbor degree. However, deviations of other graph theoretical measures between model and empirical network are indicative of genuine higher-order patterns, like clustering or rich clubs, not simply accountable by the degree sequence alone [14, 15].

III. SPECTRAL ENTROPIES FRAMEWORK

A measure of complexity is central to the understanding of differences and similarities between networks, and to decode the information that they represent. Supported by the seminal demonstration that the von Neumann entropy of a properly defined density matrix may be used for network comparison [7], in this paper we address the unsolved problem of inverse temperature selection and show that the model fitting strongly depends on it.

The first observation that an appropriately normalized graph Laplacian can be treated as a density matrix of a quantum system, is credited to the authors of reference [16]. Indeed, the Laplacian spectrum encloses a number of important topological properties of the graph [17–19]. For instance, the multiplicity of the zero eigenvalue corresponds to the number of connected components, the multiplicity of each eigenvalue is related to graph symmetries [19], the concept of expanders and isoperimetric number are connected to the first and second largest eigenvalues [20, 21]. Moreover, the graph Laplacian appears often in the study of random walkers [22, 23], diffusion [24], combinatorics [25] and a large number of other applications [19, 25].

After the first demonstration that a graph can be always represented as a uniform mixture of pure density matrices [16], at least two different definitions of quantum density for complex networks have been used [7, 26].

Adopting the notation of quantum physics, the von Neumann density matrix ρ is a Hermitian and positive semidefinite matrix with unitary trace, that admits a spectral decomposition as:

$$\rho = \sum_{i=1}^n \lambda_i(\rho) |\phi_i\rangle \langle \phi_i| \quad (2)$$

for an orthonormal basis $\{|\phi_i\rangle\}$ and eigenvalues $\lambda_i(\rho)$. Thus, a density matrix can be represented as a convex combination of pure states [26].

The von Neumann entropy of the density operator ρ can be expressed as the Shannon entropy of its eigenvalues [27]:

$$S(\rho) = -\text{Tr}[\rho \log \rho] = -\sum_{i=1}^n \lambda_i(\rho) \log \lambda_i(\rho) \quad (3)$$

where $\log(\cdot)$ is the principal matrix logarithm [28] when the argument is a matrix. The von Neumann entropy of the density matrix is bounded between 0 and $\log n$ [27].

We adopt the quantum statistical mechanics perspective [7], where the von Neumann density matrix ρ of a complex network is built considering a quantum system with Hamiltonian \mathbf{L} in thermal contact with a heat bath at constant temperature $k_B T = 1/\beta$, where k_B is the Boltzmann constant. The resulting density matrix ρ is described by the quantum Gibbs-Boltzmann distribution:

$$\rho = \frac{e^{-\beta \mathbf{L}}}{\text{Tr}[e^{-\beta \mathbf{L}}]}, \quad (4)$$

where here $e^{(\cdot)}$ is the matrix exponential when the argument is a matrix and the denominator is the so-called partition function of the system, i.e. the sum over all possible configurations of the ensemble, and is denoted by $Z = \text{Tr}[e^{-\beta \mathbf{L}}]$. From the terminology of statistical physics, thermal averages of any graph-theoretical measure \mathbf{O} are:

$$\langle \mathbf{O} \rangle_\rho = \text{Tr}[\mathbf{O} \rho] = \frac{1}{Z} \text{Tr}[\mathbf{O} e^{-\beta \mathbf{L}}]. \quad (5)$$

The choice of this density matrix for complex networks is supported by the observation that previous definitions of entropy [16, 26] in graph theory resulted in violation of sub-additivity [7, 29], a central property of entropy [27]. The strength of this definition of von Neumann entropy for graphs lies in the possibility to establish a connection between quantum statistical mechanics and the realm of networks. Moreover, this approach closely resembles the one taken in the study of diffusion on networks [23], where β is no longer interpreted as an inverse temperature of the external heat bath, but rather as the diffusion time of a random walker [30, 31]. This renders the idea

that the network properties can be explored at different scales by varying β [23, 29, 32].

The application of the previously introduced concepts from information theory and statistical mechanics to complex networks can offer many intriguing possibilities, the most important one being the quantification of the amount of shared information between graphs. Moreover, it is possible to fit a model with a density matrix $\sigma(\theta)$ to an observed network described by an empirical density matrix ρ by means of spectral entropies.

The relative entropy, or Kullback-Leibler divergence $D_{KL}(\rho \parallel \sigma)$ between two density matrices ρ and σ is a nonnegative quantity that measures the expected amount of information lost when σ is used instead of ρ [7, 27, 33]. In this context, we quantify the Kullback-Leibler divergence between complex networks as:

$$D_{KL}(\rho \parallel \sigma) = \text{Tr}[\rho(\log \rho - \log \sigma)] \geq 0. \quad (6)$$

From the linearity of the trace operator, it is apparent that Eq. (6) consists of two terms. The first term is the negative value of entropy of the empirical density ρ . The second term $\log \mathcal{L} = -\text{Tr}[\rho \log \sigma]$ can be seen as the expected log-likelihood ratio between densities ρ and σ [7, 27, 33, 34]. For this reason we can also express Eq. (6) as:

$$D_{KL}(\rho \parallel \sigma) = -S(\rho) - \log \mathcal{L}(\rho, \sigma(\theta)). \quad (7)$$

Indeed Eq. (7) can be thought as a measure to quantify the discrepancy between observation and model. Hence, it can define a function to be minimized in a fitting procedure of a model $\sigma(\theta)$ to the data ρ . However, to obtain a robust estimate of the matrix σ , one should average over many realizations of σ . While this could be achieved via Monte-Carlo sampling, it is not practical. Importantly, in this case one cannot use continuous optimization techniques as the log-likelihood landscape is not smooth, and only slow global optimization methods such as simulated annealing or genetic algorithms are suitable, with no theoretical guarantee of robust estimates of model parameters. However, for generative models with continuous dependency over their parameters, it is possible to analytically construct the density matrix σ . In these general settings we can apply continuous optimization techniques relying on the analytically computed gradients:

$$\frac{\partial D_{KL}}{\partial \theta} = \beta \text{Tr} \left[(\rho - \sigma(\theta)) \frac{\partial \mathbf{L}_\sigma(\theta)}{\partial \theta} \right], \quad (8)$$

where $\mathbf{L}_\sigma(\theta)$ is the Laplacian of the model (see Appendix A for detailed calculation). This last equation is the basis of the following sections as it is necessary for the application of continuous optimization methods.

A. Thermodynamic interpretation

The Klein inequality states that the quantum relative entropy of two density matrices is always non negative, and zero only in the case $\rho = \sigma$ [27]. It is interesting to rework the expression for the Kullback-Leibler divergence making use of thermodynamic quantities [8, 35]. We denote the Helmholtz free energies of the empirical network and of the model as $F_\rho = -\beta^{-1} \log Z_\rho$ and $F_\sigma = -\beta^{-1} \log Z_\sigma$, respectively. The partition functions are computed as $Z_\rho = \text{Tr} [e^{-\beta \mathbf{L}_\rho}]$, $Z_\sigma = \text{Tr} [e^{-\beta \mathbf{L}_\sigma}]$. The ensemble averages of the empirical and model Laplacians are $\langle \mathbf{L}_\rho \rangle_\rho := \text{Tr} [\rho \mathbf{L}_\rho]$ and $\langle \mathbf{L}_\sigma \rangle_\rho := \text{Tr} [\rho \mathbf{L}_\sigma]$, where $\langle \cdot \rangle_\rho$ indicates thermal averaging with respect to the canonical distribution pertaining to the observed network Laplacian \mathbf{L}_ρ . After rearrangement of the terms, the expression for the relative entropy described in Eq. (6) becomes:

$$D_{KL}(\rho \parallel \sigma) = \beta [(F_\rho - F_\sigma) - (\langle \mathbf{L}_\rho \rangle_\rho - \langle \mathbf{L}_\sigma \rangle_\rho)] \geq 0. \quad (9)$$

Clearly, the Klein inequality implies the following condition, also known as Gibbs' inequality in statistical physics [35]:

$$\langle \mathbf{L}_\sigma \rangle_\rho - F_\sigma \geq \langle \mathbf{L}_\rho \rangle_\rho - F_\rho \quad (10)$$

This expression has a profound physical interpretation [8, 35, 36]. Let us consider a system with Hamiltonian $\mathbf{L}_\sigma(\theta^*)$ where the parameters θ^* are given. This system is in equilibrium at temperature $1/\beta$ with a heat bath and its density matrix is $\sigma^* = \sigma(\theta^*)$. Suppose we are given a sampling procedure to create real networks from the system described by the density σ^* . Naturally, the properties of a sampled network will slightly deviate from its ensemble averages. Indeed, except for a few trivial cases, the density ρ of a single network sampled from σ^* will never be perfectly equal to σ^* .

Thus, the generation of a random graph instance given a model described by Hamiltonian \mathbf{L}_σ can be interpreted as a sudden perturbation where the Hamiltonian of the system is driven from \mathbf{L}_σ to \mathbf{L}_ρ . In the general case this corresponds to an irreversible transformation, except for graphs where there are no possible rewirings preserving the given constraints, up to node permutations.

In this sense, minimization of the relative entropy is equivalent to finding a set of parameters $\tilde{\theta}$ such that the work required to bring the system described by ρ to a state $\sigma(\tilde{\theta})$ is minimum. However $\tilde{\theta}$ is not guaranteed to be equal to θ^* due to irreversibility of the sampling. In order to precisely reconstruct the parameters $\tilde{\theta} = \theta^*$, minimization of relative entropy averaged over the whole set of samples is therefore needed. The Taylor expansion in Eq. (11) of the gradients (8) reflects the fact that for

$\beta > 0$, null gradients do not necessarily imply the equality of the energies of the two systems, defined by $\text{Tr} [\mathbf{L}]$. Put in other terms, they do not necessarily have the same number of links, which is the first desired property for reconstruction.

$$\begin{aligned} \frac{\partial D_{KL}}{\partial \theta} \approx & \frac{\beta^2}{n^2} \text{Tr} \left[\frac{\partial \mathbf{L}_\sigma}{\partial \theta} \right] \text{Tr} [\mathbf{L}_\rho - \mathbf{L}_\sigma] - \\ & - \frac{\beta^2}{n} \text{Tr} \left[(\mathbf{L}_\rho - \mathbf{L}_\sigma) \frac{\partial \mathbf{L}_\sigma}{\partial \theta} \right]. \end{aligned} \quad (11)$$

Intriguingly, only linear terms in the Laplacians appear in this low order expansion of the gradients. Taking the further orders of the gradients of D_{KL} (see appendix C), higher powers of \mathbf{L}_ρ and \mathbf{L}_σ are compared. Hence, relative entropy measures differences of complex patterns on scales determined by β , which acts as a hyper-parameter for the minimization problem.

The exponential random graph models presented so far are designed to eliminate node correlations that are not explained by the constrained properties alone. For example in the UBCM, one looks for the maximally random ensemble of networks with a given degree sequence: nodal correlations other than those emerging from the degree sequence are not explicitly specified.

The inverse temperature β plays the role of a resolution parameter allowing one to compare two networks at different scales [7, 29]. Therefore, for the ERGM, the optimal β has to go to zero, as we are comparing the lowest order properties of the networks, linearly dependent on the adjacency matrix. On the other hand, for β tending to zero, the two density matrices ρ and σ tend to identity, so any choice of the parameters trivially yields zero relative entropy. Hence, to guide the optimization towards a non-trivial solution, one must start with some initial guess of β_0 , isothermically find a local minimum, and afterwards decrease β . Eventually, as β tends to zero, the optimal solution will change slowly while making the relative entropy as small as possible. Here, for the Erdős-Rényi and the planted partition model, we show analytically that correct reconstruction of the empirical density parameters is possible only in the limit $\beta \rightarrow 0$.

B. Erdős-Rényi random graph

The Erdős-Rényi random graph is the simplest example of random graph model [11]. Each pair of nodes is connected by a link with constant probability p . In this case it is possible to analytically find the optimum solution for the problem of relative entropy minimization. The partition function $Z_\sigma(n, p)$ and the free energy of the

model $F_\sigma(n, p, \beta)$ are:

$$Z_\sigma(p) = (n-1)e^{-n\beta p} + 1 \quad (12)$$

$$\text{Tr}[\mathbf{L}_\sigma(p)\rho] = p(n - R(n, \beta)), \quad (13)$$

where $R(n, \beta) = \text{Tr}[\mathbf{1}\rho] = \sum_{i,j}^n \rho_{ij}$ is the grand sum of density matrix. Both Z_ρ and F_ρ are observation dependent quantities and must be evaluated numerically from the observed network. Finding the minimum of the left hand side of Eq. (10) corresponds to setting to zero the derivative with respect to p :

$$\begin{aligned} \frac{\partial}{\partial p} \left(\text{Tr}[\mathbf{L}_\sigma(p)\rho] + \frac{\log Z_\sigma(p)}{\beta} \right) &= 0 \\ &= \text{Tr} \left[\frac{\partial \mathbf{L}_\sigma(p)}{\partial p} \rho \right] - \frac{n(n-1)}{e^{\beta np} + (n-1)} = 0 \end{aligned} \quad (14)$$

Solving for p we can find an analytical expression for the optimal density \tilde{p} that can be reconstructed by the model:

$$\tilde{p} = \frac{1}{n\beta} \log \left[\frac{R(n, \beta)(n-1)}{(n - R(n, \beta))} \right]. \quad (15)$$

The reconstruction of the observed empirical density $p^* = 2m^*/(n(n-1))$ is only possible in the limit $\beta \rightarrow 0$. It can be shown, with the help of computer algebra system, that:

$$\lim_{\beta \rightarrow 0} \tilde{p} = p^* = \frac{2m^*}{n(n-1)}. \quad (16)$$

We also extended the same calculations to the *planted-partition* model, the simplest extension of the Erdős-Rényi model to networks presenting a community structure [37].

C. Planted partition model

In the planted partition model, the nodal block membership vector $c_i \in \mathbb{N}$ specifies to which community the node i belongs and it has the role of a hyper-parameter. The model parameters are the intrablock and interblock link densities p_{in} and p_{out} . The adjacency matrix \mathbf{A}_σ and the Laplacian \mathbf{L}_σ are:

$$\mathbf{A}_\sigma = \delta p_{\text{in}} + (\mathbf{1} - \delta)p_{\text{out}} \quad (17)$$

$$\begin{aligned} \mathbf{L}_\sigma = \mathbf{I} &(p_{\text{in}}(n/b - 1) + p_{\text{out}}(n/b)(b - 1)) - \\ &- \delta p_{\text{in}} - (\mathbf{1} - \delta)p_{\text{out}}, \end{aligned} \quad (18)$$

where $\delta = \{\delta_{c_i, c_j}\}$ is the block assignment matrix, $\mathbf{1}$ is the matrix of ones and \mathbf{I} is the identity matrix. Analogous calculations as in the Erdős-Rényi case can be analytically performed in the planted partition model with exactly b

blocks of the same size. In this case the partition function of the model $Z_\sigma(p_{\text{in}}, p_{\text{out}})$ becomes:

$$\begin{aligned} Z_\sigma(p_{\text{in}}, p_{\text{out}}) &= \text{Tr} \left[e^{-\beta \mathbf{L}_\sigma} \right] = \\ &= (n-b) \exp \left[-\beta n (p_{\text{in}} + (b-1)p_{\text{out}}) / b \right] + \\ &+ (b-1) \exp \left[-\beta np_{\text{out}} \right] + 1. \end{aligned} \quad (19)$$

Setting the gradients of relative entropy (8) to zero, results in a system of two equations:

$$\begin{cases} \text{Tr} \left[\frac{\partial \mathbf{L}_\sigma}{\partial p_{\text{in}}} \rho \right] + \frac{1}{\beta} \frac{\partial \log Z_\sigma}{\partial p_{\text{in}}} = 0 \\ \text{Tr} \left[\frac{\partial \mathbf{L}_\sigma}{\partial p_{\text{out}}} \rho \right] + \frac{1}{\beta} \frac{\partial \log Z_\sigma}{\partial p_{\text{out}}} = 0. \end{cases} \quad (20)$$

An analytical solution is possible for $b = 2$ blocks:

$$\tilde{p}_{\text{in}} = \frac{1}{\beta n} \log \left[\frac{(n-2)^2 R(2Q - R)}{(n-2Q)^2} \right] \quad (21)$$

$$\tilde{p}_{\text{out}} = \frac{1}{\beta n} \log \left[\frac{R}{2Q - R} \right] \quad (22)$$

where R is the grand-sum of ρ and $Q := Q(n, b, \beta) = \text{Tr}[\delta\rho]$. The empirical intra-block and inter-block densities p_{in}^* and p_{out}^* can be reconstructed only in the limit of infinite temperature:

$$\begin{aligned} \lim_{\beta \rightarrow 0} \tilde{p}_{\text{in}} &= p_{\text{in}}^* \\ \lim_{\beta \rightarrow 0} \tilde{p}_{\text{out}} &= p_{\text{out}}^*. \end{aligned} \quad (23)$$

Unfortunately, though, the calculations performed for these two last examples cannot be straightforwardly extended to the configuration model (UBCM) and other more complex variants of the exponential random graph model, as the expression of the whole partition function Z_σ for general models is too complex for a fully analytical treatment. Therefore, we rely on numerical simulations to show that the limit $\beta \rightarrow 0$ yields a correct reconstruction of model parameters for the UBCM.

D. Configuration model

In the Undirected binary configuration model (UBCM) the model parameters are the hidden variables $\mathbf{x} = \{x_i\}$. Given some network with fixed degree sequence, we can consider its Laplacian \mathbf{L}_ρ as the Laplacian of a graph sampled from the UBCM ensemble.

Importantly, being \mathbf{L}_ρ a realization of a random graph ensemble, we cannot expect to be able to reconstruct exactly the parameters \mathbf{x}^* which generated that network.

As a demonstration of this concept we generated a random network with $n = 40$ nodes and a degree sequence sampled from the uniform distribution.

Starting from a random solution $\mathbf{x}(t_0, \beta_0)$, we minimized the relative entropy at an initial guess of $\beta_0 \gg 1$ to obtain the new solution $\mathbf{x}(t_1, \beta_0)$. This procedure was repeated gradually decreasing β at each iteration, until the solution was not changing considerably, for β close to 0.

As a measure of convergence, we chose the difference of the total number of links, which in thermodynamic interpretation equals to the difference of the total energies: $\Delta m = (\text{Tr}[\mathbf{L}_\sigma] - \text{Tr}[\mathbf{L}_\rho])/2$. The bigger the absolute value of Δm , the less similar the empirical network is from the average realization of the ensemble.

In Figure 1A we plotted the spectral entropies of the empirical network (red line) and the fitted model at optimal solution $\tilde{\mathbf{x}}$ (blue line) as a function of β . Figure 1B shows the difference in the number of links Δm as a function of β . At the optimal solution for $\beta \rightarrow 0$, there is a small deviation in total number of links ($\Delta m \approx -3.64$). This is explained by the irreversibility of the sampling process, that implies inability to precisely reconstruct the true parameters \mathbf{x}^* from only one sample. However, the deviation of the reconstructed parameters $\tilde{\mathbf{x}}$ from \mathbf{x}^* can be reduced with enough samples of the random graph ensemble, as shown in Figure 1 (panels C and D).

As a second example we chose a toy network consisting of a number of cliques of increasing size connected in a ring, and one of its degree-preserving random rewiring (Figure 2C,F). In the ordered case, the clique structure cannot be accounted by a first-order average model alone, making that specific instance highly unlikely when sampling from the configuration model. Therefore, following the fitting procedure described above, one can see a significant difference in the number of links between model and data Δm even at a very small beta Figure 2B. In other words, in the ordered case, the degree sequence alone cannot explain the differences in the spectral entropies, thus indicating the presence of genuine regular patterns that substantially alter the properties of diffusion of the random walk defined by the density matrix. Indeed, this difference reflects the intrinsic inability of the model to account for the characteristic structure of the underlying network.

After fitting, non vanishing Δm serves as an indicator of the presence of ordered patterns in the given network that are not explained by this model alone. To test this idea we applied the same optimization technique to the degree-preserving randomly rewired network in Figure 2F, and plotted the results in Figure 2D,E. In this case the random rewiring made the empirical network more adherent to the optimal reconstruction by the model and the difference in the total number of links at β close to zero is much smaller than in the ordered case. This is also evident by the better adherence in the spectral entropies,

as shown in Figure 2D.

IV. COMPARISON WITH CLASSICAL MAXIMUM LIKELIHOOD APPROACHES

Typically a likelihood function is defined over the space of all possible networks and evaluated for the observed one. Without loss in generality, if the model prescribes a link probability $p_{ij}(\theta)$ between node i and node j , then a realization with adjacency matrix \mathbf{A} has probability:

$$P(\mathbf{A}) = \prod_{i < j} p_{ij}^{a_{ij}} (1 - p_{ij})^{1-a_{ij}} \quad (24)$$

as every link realization is an independent Bernoulli trial. Maximization of probability (24) for a model network leads to a reconstruction of the optimal parameters θ^* . However, this expression is identical for two networks sampled from the same probability distribution p_{ij} ; therefore, in the configuration model, it is independent of a random rewiring that preserves the degree sequence [6]. Hence, the ring of cliques network and its degree-preserving rewired counterpart have the same probability under Eq. (24). For this reason, this likelihood function is not a good way to identify recurring topological motifs.

In the spectral entropy framework, the rewiring process substantially changes the density matrix, making it possible to distinguish between two different realizations of a degree preserving randomization. This property is rooted in the use of a density function based on matrix exponential. Indeed, the matrix exponential is a compact way to consider all possible powers of the adjacency matrix, and to consider all the possible paths present in the network at once.

The density matrix ρ contains all higher order topological properties, not just the degree sequence, which is only its first order approximation. This is apparent from the Taylor expansion of the density matrix (see Appendix C).

V. SPATIAL MODELS

Embedding in a two or three dimensional space has bearings on the topological properties of real-world networks. When the formation of links has a cost associated with distance, the model must accomodate additional spatial constraints, which introduce correlation between topological and geometrical organization [38]. An example is represented by neural networks, in which communication between neurons implies a metabolic cost that depends on their distance [39, 40]. The material

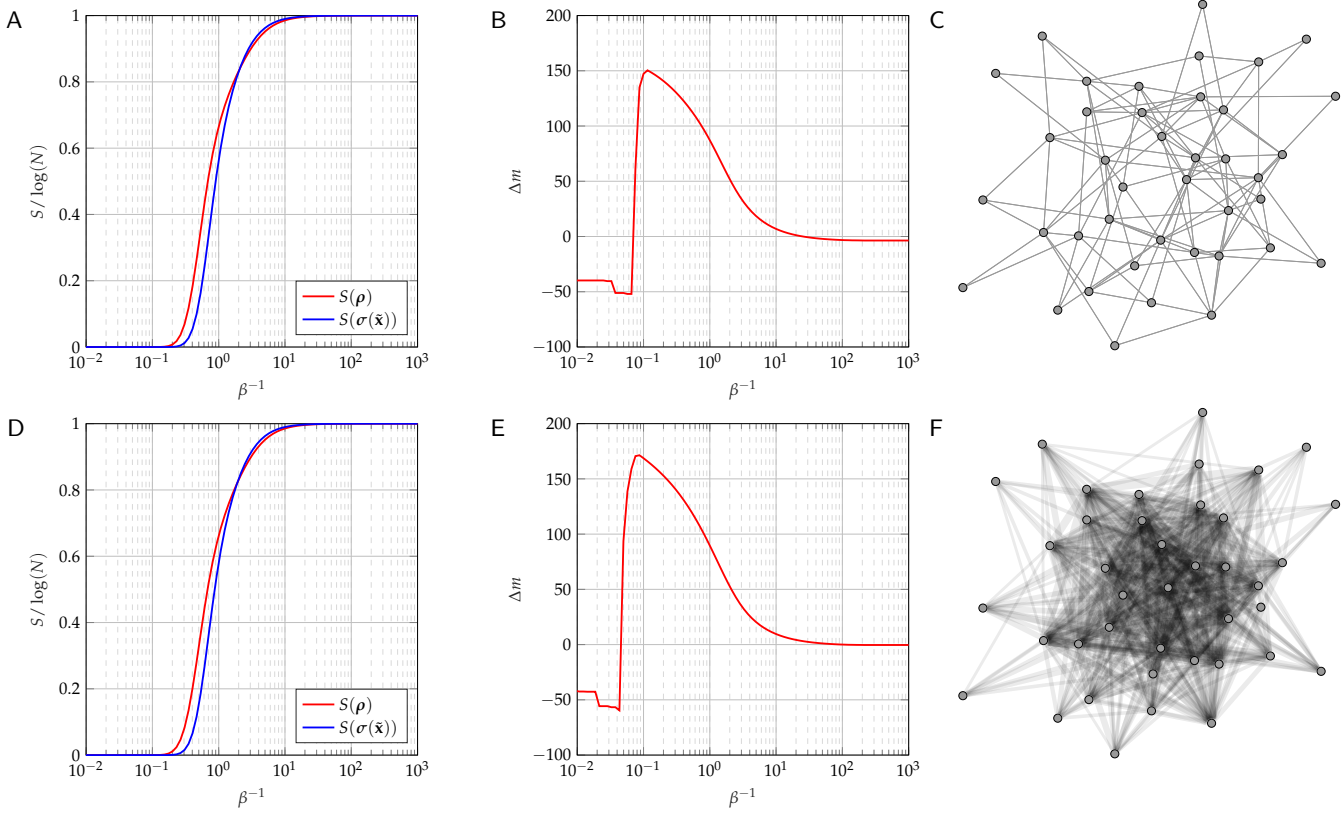


Figure 1: Normalized von Neumann entropy and reconstruction error of a random network (top panels) and its ensemble average with the same degree sequence (bottom panels). In panels A,D the red curves are the spectral entropy of the observed network described by density ρ , blue curves are the spectral entropies of the model network at optimum parameters $\sigma(\tilde{\theta})$. In panel B a systematic error exists at every β (even in the limit $\beta \rightarrow 0$): the UBCM cannot fit all the specific properties of the highly ordered network. On the other hand, an ensemble average network has a structure that can be better reconstructed by the UBCM, as shown by the error Δm going to zero in Panel E.

and metabolic constraints of neuronal wiring are factors that contributed to shaping brain architecture [39, 41, 42]. Computational and empirical studies converged on the result that a multiscale organization of modules inside modules is the one that satisfies the constraints imposed by minimization of energetic cost and spatial embedding [39, 40, 43, 44]. Here, wiring cost includes the physical volume of axons and synapses, the energetic demand for signal transmission, additional processing cost for noise correction over long distance signaling and sustenance of the necessary neuroglia that support neuronal activities [39]. Therefore, it is tempting to assume that the expected number of neural fibers between two areas could be expressed as a decreasing function of their length. With this hypothesis in mind, we verified the ability of our approach to work with a simple generative model describing the observed neural connectivity in the macaque cortex [45, 46]. The model called Exponential Distance Rule (EDR) describes the decline in the expected number of axonal projections w_{ij} as a func-

tion of the inter-areal distances d_{ij} and a tunable decay parameter ℓ :

$$\langle w_{ij} \rangle = C e^{-\ell d_{ij}}, \quad (25)$$

where C is a normalization constant. Here, the distances d_{ij} are measured along the shortest path connecting areas via white matter, approximating the axonal distance [45].

We used a dataset of cortico-cortical connectivity generated from retrograde tracing experiments in the macaque brain [45, 46]. Following the procedure introduced in the previous sections, we fitted the macaque connectome network with the EDR model. Differently from the random graph models described in previous sections, we found an optimal inverse-temperature parameter β that minimizes the reconstruction error, as shown in Figure 3B. At this optimal $\beta^* \approx 3.05$ the reconstructed decay parameter $\ell = 0.1505 \text{ [mm]}^{-1}$ is comparable to the values obtained by the three methods applied in the original paper from Ref [46]. The non-vanishing difference in total weights between reconstructed and object networks

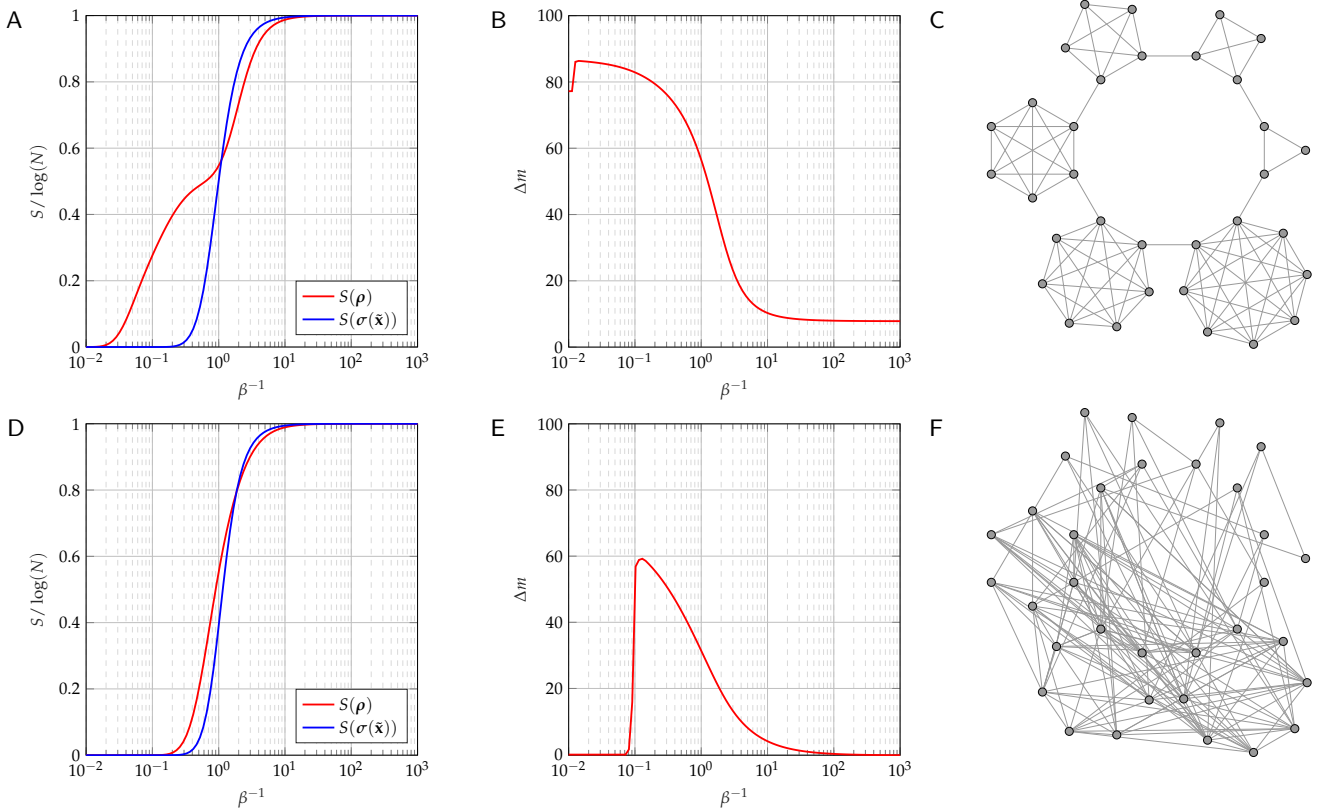


Figure 2: Normalized von Neumann entropy and reconstruction error of two networks: a ring of cliques (top panels) and its degree-preserving random rewiring (bottom panels). In panels A,D the red curves are the spectral entropy of the observed network described by density ρ , blue curves are the spectral entropies of the model network at optimum parameters $\sigma(\bar{\theta})$. In panel B a systematic error exists at every β (even in the limit $\beta \rightarrow 0$): the UBCM cannot fit all the specific properties of the highly ordered network. On the other hand, a degree preserving rewired network has a structure that can be better reconstructed by the UBCM, as shown by the error Δm going to zero in Panel E.

indicates that the model cannot account completely for the structures such as the high density core observed in the connectome [46]. A non-zero optimal value for β suggests the existence of a scale at which the model best describes the topological properties of the network.

VI. CONCLUSION

The classical maximum likelihood method to infer network model parameters relies on specific descriptors. The spectral entropy framework enables comparing networks taking into account the whole structure at multiple scales. However, this approach introduces a hyperparameter β that plays the role of an inverse temperature, and whose tuning is critical for the correct estimate of the model parameters.

Leveraging this thermodynamic analogy, we have shown that the optimal value of the hyperparameter is model dependent and reflects the scales at which the model best describes the empirical network. Moreover,

we have described procedures to determine β for the model parameter optimization.

Specifically, we focused on three examples from the exponential random graph model, namely the Erdős-Rényi, a planted partition and undirected binary configuration model. In the Erdős-Rényi model and in the planted partition model, we analytically demonstrated that correct reconstruction is possible only in the infinite temperature limit. In the configuration model this hypothesis was verified numerically. The presence of ordered structures unaccounted for by the model is reflected in a bias of the total energy, corresponding to the total number of links in the reconstructed network.

Motivated by these findings in synthetic networks, we applied the spectral entropy framework to a real-world network of the macaque brain structural connectome. A structural connectome is a spatial network whose development is thought to be constrained by geometrical and wiring cost factors. Hence, we evaluated an exponential distance rule model that assumes that the weight of inter-

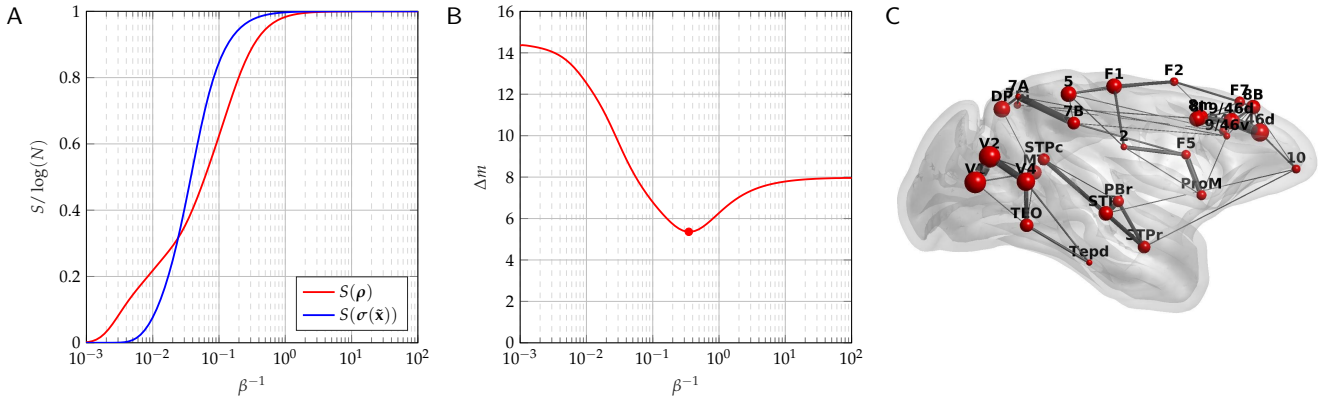


Figure 3: Normalized von Neumann entropy and reconstruction error of the macaque brain connectivity network (panel C). In panel A the red curve is the spectral entropy of the observed network described by density ρ , blue curve is the spectral entropy of the model network at optimum parameter $\sigma(\bar{\theta})$. The optimal hyperparameter β is found in panel B where the reconstruction error Δm achieve its minimum denoted by a red dot. Brain area abbreviations are specified in Appendix D.

areal connections is a decreasing function of distance. We demonstrate the existence of a non-zero optimal value of β for the computation of model parameters. However, the residual energy bias indicates the network structure at certain scales cannot be described by the exponential distance rule model alone.

The procedures demonstrated here make it possible to use relative entropy methods for practical applications to the study of models of real-world networks.

ACKNOWLEDGEMENTS

This project has received funding from the European Union's Horizon 2020 Research and Innovation Program under grant agreement No 668863.

Appendix A: Gradients of the relative entropy

Here we present a step-by-step analytical calculation of the gradients of the log-likelihood function described in the main text. We begin by observing that the matrix logarithm of the model density $\sigma(\theta)$ can be expressed as the difference of two terms:

$$\log \sigma(\theta) = \log \left(e^{-\beta \mathbf{L}(\theta)} \right) - \log \left(\text{Tr} \left[e^{-\beta \mathbf{L}(\theta)} \right] \right) \mathbf{I} \quad (\text{A1})$$

where \mathbf{I} is the $n \times n$ identity matrix. For positive definite matrices it is possible to identify the first summand in the right hand side of Eq. (A1) as equal to $-\beta \mathbf{L}(\theta)$. Thus, the log-likelihood function reads:

$$-\log \mathcal{L}(\rho, \sigma(\theta)) = -\text{Tr} \left[\rho \left(-\beta \mathbf{L}(\theta) - \log \left(\text{Tr} \left[e^{-\beta \mathbf{L}(\theta)} \right] \right) \mathbf{I} \right) \right] \quad (\text{A2})$$

By the linearity of the trace operator the derivatives of Eq. (A2) are:

$$\begin{aligned} -\frac{\partial \mathcal{L}}{\partial \theta} &= -\frac{\partial \text{Tr} [\rho \log \sigma(\theta)]}{\partial \theta} = \\ &= -\text{Tr} \left[\rho \frac{\partial}{\partial \theta} \left(-\beta \mathbf{L}(\theta) - \log \left(\text{Tr} \left[e^{-\beta \mathbf{L}(\theta)} \right] \right) \mathbf{I} \right) \right] = \\ &= -\text{Tr} \left[\rho \left(-\beta \frac{\partial \mathbf{L}(\theta)}{\partial \theta} - \frac{\mathbf{I}}{\text{Tr} [e^{-\beta \mathbf{L}(\theta)}]} \frac{\partial}{\partial \theta} \left(\text{Tr} \left[e^{-\beta \mathbf{L}(\theta)} \right] \right) \right) \right] = \\ &= \beta \text{Tr} \left[\rho \frac{\partial \mathbf{L}(\theta)}{\partial \theta} \right] + \frac{1}{\text{Tr} [e^{-\beta \mathbf{L}(\theta)}]} \frac{\partial}{\partial \theta} \text{Tr} \left[e^{-\beta \mathbf{L}(\theta)} \right] \quad (\text{A3}) \end{aligned}$$

For the sake of clarity, we compute the last term of Eq. (A3) separately. The following identity holds for the derivatives of the exponential map:

$$\begin{aligned} \frac{d}{dt} \text{Tr} \left[e^{\mathbf{X}(t)} \right] &= \text{Tr} \left[\frac{d}{dt} e^{\mathbf{X}(t)} \right] = \\ &= \text{Tr} \left[\int_0^1 e^{\alpha \mathbf{X}(t)} \frac{d\mathbf{X}}{dt} e^{(1-\alpha) \mathbf{X}(t)} d\alpha \right] = \\ &= \int_0^1 \text{Tr} \left[e^{\alpha \mathbf{X}(t)} \frac{d\mathbf{X}}{dt} e^{(1-\alpha) \mathbf{X}(t)} \right] d\alpha = \\ &= \int_0^1 \text{Tr} \left[e^{(1-\alpha) \mathbf{X}(t)} e^{\alpha \mathbf{X}(t)} \frac{d\mathbf{X}}{dt} \right] d\alpha = \\ &= \int_0^1 \text{Tr} \left[e^{\mathbf{X}(t)} \frac{d\mathbf{X}}{dt} \right] d\alpha = \\ &= \text{Tr} \left[e^{\mathbf{X}(t)} \frac{d\mathbf{X}}{dt} \right] \quad (\text{A4}) \end{aligned}$$

Applying the identity (A4) we get:

$$\frac{\partial}{\partial \theta} \text{Tr} \left[e^{-\beta \mathbf{L}(\theta)} \right] = \text{Tr} \left[e^{-\beta \mathbf{L}(\theta)} \frac{\partial(-\beta \mathbf{L}(\theta))}{\partial \theta} \right] = \quad (\text{A5})$$

$$= -\beta \text{Tr} \left[e^{-\beta \mathbf{L}(\theta)} \frac{\partial \mathbf{L}(\theta)}{\partial \theta} \right] \quad (\text{A6})$$

Finally, collecting all the terms together, we obtain a closed-form expression for the gradient of the log-likelihood:

$$-\frac{\partial \log \mathcal{L}}{\partial \theta} = \beta \text{Tr} \left[\rho \frac{\partial \mathbf{L}(\theta)}{\partial \theta} \right] - \quad (\text{A7})$$

$$\begin{aligned} & -\beta \frac{1}{\text{Tr} [e^{-\beta \mathbf{L}(\theta)}]} \text{Tr} \left[e^{-\beta \mathbf{L}(\theta)} \frac{\partial \mathbf{L}(\theta)}{\partial \theta} \right] = \\ & = \beta \text{Tr} \left[\rho \frac{\partial \mathbf{L}(\theta)}{\partial \theta} \right] - \beta \text{Tr} \left[\sigma(\theta) \frac{\partial \mathbf{L}(\theta)}{\partial \theta} \right] = \\ & = \beta \text{Tr} \left[(\rho - \sigma(\theta)) \frac{\partial \mathbf{L}(\theta)}{\partial \theta} \right] \end{aligned} \quad (\text{A8})$$

Appendix B: Thermodynamic interpretation of relative entropy

The relative entropy Eq. (6) can be written as:

$$\begin{aligned} D_{KL}(\rho \parallel \sigma) &= \text{Tr} [\rho \log \rho] - \text{Tr} [\rho \log \sigma] = \\ &= \text{Tr} \left[\rho \left(-\beta \mathbf{L}_\rho - \log \left(\text{Tr} [e^{-\beta \mathbf{L}_\rho}] \right) \mathbf{I} \right) \right] - \\ &\quad - \text{Tr} \left[\rho \left(-\beta \mathbf{L}_\sigma - \log \left(\text{Tr} [e^{-\beta \mathbf{L}_\sigma}] \right) \mathbf{I} \right) \right]. \end{aligned} \quad (\text{B1})$$

Interestingly, we note that this expression contains the partition functions Z_ρ and Z_σ for the observed and model networks as well as the ensemble averages $\langle \mathbf{L}_\rho \rangle_\rho$ and $\langle \mathbf{L}_\sigma \rangle_\rho$:

$$\begin{aligned} Z_\rho &= \text{Tr} \left[e^{-\beta \mathbf{L}_\rho} \right], & Z_\sigma &= \text{Tr} \left[e^{-\beta \mathbf{L}_\sigma} \right], \\ \langle \mathbf{L}_\rho \rangle_\rho &= \text{Tr} [\mathbf{L}_\rho \rho] & \langle \mathbf{L}_\sigma \rangle_\rho &= \text{Tr} [\mathbf{L}_\sigma \rho]. \end{aligned}$$

With these definitions, we rewrite the relative entropy in thermodynamic terms as:

$$D_{KL}(\rho \parallel \sigma) = -\beta \langle \mathbf{L}_\rho \rangle_\rho - \log Z_\rho + \beta \langle \mathbf{L}_\sigma \rangle_\rho + \log Z_\sigma, \quad (\text{B2})$$

where $\text{Tr} [\rho] = 1$. Denoting F_ρ and F_σ as the Helmholtz free energies

$$F_\rho = -\frac{\log Z_\rho}{\beta}, \quad F_\sigma = -\frac{\log Z_\sigma}{\beta} \quad (\text{B3})$$

we obtain an expression that highlights in thermodynamic terms the relation between relative entropy and the Gibbs inequality:

$$D_{KL}(\rho \parallel \sigma) = \beta \left[(F_\rho - F_\sigma) - (\langle \mathbf{L}_\rho \rangle_\rho - \langle \mathbf{L}_\sigma \rangle_\rho) \right] \geq 0. \quad (\text{B4})$$

Appendix C: Second order expansions

In the limit $\beta \ll 1$, the second order expansion of the density matrix is:

$$\begin{aligned} \rho &\approx \frac{\mathbf{I}}{n} - \beta \frac{\mathbf{L}_\rho}{n} + \beta \mathbf{I} \frac{\text{Tr} [\mathbf{L}_\rho]}{n^2} + \\ &\quad + \frac{\beta^2}{n} \left(\mathbf{I} \left(\frac{(\text{Tr} [\mathbf{L}_\rho])^2}{n^2} - \frac{\text{Tr} [\mathbf{L}_\rho^2]}{2n} \right) + \frac{\mathbf{L}_\rho^2}{2} - \frac{\mathbf{L}_\rho \text{Tr} [\mathbf{L}_\rho]}{n} \right) \end{aligned} \quad (\text{C1})$$

and the gradients of the log-likelihood are:

$$\begin{aligned} \frac{\partial \log \mathcal{L}}{\partial \theta} &\approx -\frac{\beta^2}{n^2} \text{Tr} \left[\frac{\partial \mathbf{L}_\sigma}{\partial \theta} \right] \text{Tr} [\mathbf{L}_\rho - \mathbf{L}_\sigma] + \\ &\quad + \frac{\beta^2}{n} \text{Tr} \left[(\mathbf{L}_\rho - \mathbf{L}_\sigma) \frac{\partial \mathbf{L}_\sigma}{\partial \theta} \right] + \\ &\quad + \frac{\beta^3}{n} \left(\text{Tr} \left[\frac{\partial \mathbf{L}_\sigma}{\partial \theta} \right] \left(\frac{(\text{Tr} [\mathbf{L}_\rho])^2 - (\text{Tr} [\mathbf{L}_\sigma])^2}{n^2} - \right. \right. \\ &\quad \left. \left. - \frac{\text{Tr} [\mathbf{L}_\rho^2] - \text{Tr} [\mathbf{L}_\sigma^2]}{2n} \right) + \text{Tr} \left[\frac{\mathbf{L}_\rho^2 - \mathbf{L}_\sigma^2}{2} \frac{\partial \mathbf{L}_\sigma}{\partial \theta} \right] - \right. \\ &\quad \left. - \text{Tr} \left[\frac{\mathbf{L}_\rho \text{Tr} [\mathbf{L}_\rho] - \mathbf{L}_\sigma \text{Tr} [\mathbf{L}_\sigma]}{n} \frac{\partial \mathbf{L}_\sigma}{\partial \theta} \right] \right). \end{aligned} \quad (\text{C2})$$

Appendix D: List of brain areas

Experimental connectivity data for the macaque brain was taken from Ref. [45], internodal distances were taken from Ref. [46]. The list of the abbreviation of the brain regions (from Ref. [45]) is: 2 - somatosensory area 2; 5 - somatosensory area 5; 7A - area 7A; 7B - area 7B; 7m - area 7m; 8B - area 8B; 8l - lateral part of area 8; 8m - medial part of area 8; 9/46d - area 9/46, dorsal part; 9/46v - area 9/46, ventral part; 10 - area 10; 24c - area 24c; 46d - area 46, dorsal part; DP - dorsal prelunate area; F1 - frontal area F1; F2 - frontal area F2; F5 - frontal area F5; F7 - frontal area F7; MT - middle temporal area; PBr - parabelt, rostral part; ProM - area ProM; STPc - superior temporal polysensory, caudal part; STPi - superior temporal polysensory, intermediate part; STPr - superior temporal polysensory, rostral part; TEO - area TEO; TEpd - area TE, posterior-dorsal part; V1 - visual area 1; V2 - visual area 2; V4 - visual area 4.

[1] Mark Newman. *Networks: An Introduction*. OUP Oxford, 2010.

[2] Albert-Laszlo Barabasi and Reka Albert. Emergence of scaling in random networks. *Science*, 286(5439):509–512, 1999.

[3] Guido Caldarelli. *Scale-free networks: complex webs in nature and technology*. Oxford University Press, 2007.

[4] Ed Bullmore and Olaf Sporns. Complex brain networks: graph theoretical analysis of structural and functional systems. *Nat. Rev. Neurosci.*, 10(3):186–198, 2009. ISSN 1471-0048.

[5] Stanley Wasserman and Katherine Faust. *Social network analysis: Methods and applications*, volume 8. Cambridge university press, 1994.

[6] Tiziano Squartini and Diego Garlaschelli. *Maximum-Entropy Networks: Pattern Detection, Network Reconstruction and Graph Combinatorics*. Springer, 2017.

[7] Manlio De Domenico and Jacob Biamonte. Spectral entropies as information-theoretic tools for complex network comparison. *Phys. Rev. X*, 041062:1–13, 2016.

[8] Juan M.R. Parrondo, Jordan M. Horowitz, and Takahiro Sagawa. Thermodynamics of information. *Nat. Phys.*, 11(2):131–139, 2015.

[9] Juyong Park and M. E. J. Newman. Statistical mechanics of networks. *Phys. Rev. E*, 70(6):066117, 2004.

[10] E. T. Jaynes. Information theory and statistical mechanics. *Phys. Rev.*, 106(4):620–630, 1957.

[11] P Erdős and a Rényi. On random graphs. *Publ. Math.*, 6: 290–297, 1959. ISSN 00029947.

[12] G. Caldarelli, A. Capocci, P. De Los Rios, and M. A. Muñoz. Scale-free networks from varying vertex intrinsic fitness. *Phys. Rev. Lett.*, 89:258702, 2002.

[13] Tiziano Squartini, Rossana Mastrandrea, and Diego Garlaschelli. Unbiased sampling of network ensembles. *New J. Phys.*, 17(2):023052, 2015. ISSN 1367-2630.

[14] Tiziano Squartini and Diego Garlaschelli. Jan Tinbergen’s legacy for economic networks: from the gravity model to quantum statistics. *Econophysics of Agent-Based Models*, pages 161–186, 2014.

[15] Diego Garlaschelli and Maria I. Loffredo. Maximum likelihood: Extracting unbiased information from complex networks. *Phys. Rev. E*, 78(1):1–4, 2008.

[16] Samuel L. Braunstein, Sibasish Ghosh, and Simone Severini. The Laplacian of a graph as a density Matrix: A basic combinatorial approach to separability of mixed states. *Ann. Comb.*, 10(3):291–317, 2006.

[17] Ernesto Estrada. *The Structure of Complex Networks: Theory and Applications*. Oxford University Press, Inc., New York, NY, USA, 2011.

[18] William N Anderson. Eigenvalues of the Laplacian of a graph. *Linear Multilinear A.*, 18(2):141–145, 1985.

[19] Russell Merris. Laplacian matrices of graphs: a survey. *Linear Algebra Appl.*, 197–198(C):143–176, 1994.

[20] Jeff Cheeger. A lower bound for the smallest eigenvalue of the laplacian. *Problems in analysis*, pages 195–199, 1970.

[21] Luca Donetti, Franco Neri, and Miguel A Muñoz. Optimal network topologies: expanders, cages, Ramanujan graphs, entangled networks and all that. *J. Stat. Mech-Theory E*, 2006(08):P08007, 2006.

[22] L Lovász. Random walks on graphs: A survey. *Bolyai Math. Stud.*, 2(Volume 2):1–46, 1993.

[23] Naoki Masuda, Mason A. Porter, and Renaud Lambiotte. Random walks and diffusion on networks. *Phys. Rep.*, 2017.

[24] A. J. Bray and G. J. Rodgers. Diffusion in a sparsely connected space: A model for glassy relaxation. *Phys. Rev. B*, 38(16):11461–11470, 1988.

[25] Bojan Mohar, Y Alavi, G Chartrand, and OR Oellermann. The laplacian spectrum of graphs. *Graph theory, combinatorics, and applications*, 2(871-898):12, 1991.

[26] Kartik Anand, Ginestra Bianconi, and Simone Severini. Shannon and von Neumann entropy of random networks with heterogeneous expected degree. *Phys. Rev. E*, 83(3): 1–8, 2011.

[27] Mark M Wilde. *Quantum information theory*. Cambridge University Press, 2013.

[28] Nicholas J Higham. *Functions of matrices: theory and computation*. SIAM, 2008.

[29] Jacob Biamonte, Mauro Faccin, and Manlio De Domenico. Complex Networks: from Classical to Quantum. *arXiv preprint arXiv:1702.08459*, 2017.

[30] Ernesto Estrada and Naomichi Hatano. Communicability in complex networks. *Phys. Rev. E*, 77(3):1–12, 2008.

[31] Mauro Faccin, Tomi Johnson, Jacob Biamonte, Sabre Kais, and Piotr Migdał. Degree Distribution in Quantum Walks on Complex Networks. *Phys. Rev. X*, 3(4):041007, 2013.

[32] Ernesto Estrada, Naomichi Hatano, and Michele Benzi. The physics of communicability in complex networks. *Phys. Rep.*, 514(3):89–119, 2012.

[33] S. Kullback and R. A. Leibler. On Information and Sufficiency. *Ann. Math. Stat.*, 22(1):79–86, 1951. ISSN 0003-4851.

[34] Thomas M. Cover and Joy A. Thomas. *Elements of Information Theory*. Wiley-Interscience, 2006.

[35] Neri Merhav. Statistical Physics and Information Theory. *Foundations and Trends in Communications and Information Theory*, 6(1-2):1–212, 2010.

[36] Sebastian Deffner and Eric Lutz. Generalized clausius inequality for nonequilibrium quantum processes. *Phys. Rev. Lett.*, 105(17):1–4, 2010.

[37] Anne Condon and Richard M Karp. on the Planted Partition Model. *Electr. Eng.*, pages 116–140, 2000.

[38] Marc Barthélémy. Spatial networks. *Phys. Rep.*, 499(1-3): 1–101, 2011.

[39] Ed Bullmore and Olaf Sporns. The economy of brain network organization. *Nat. Rev. Neurosci.*, 13(5):336–349, 2012. ISSN 1471-0048.

[40] Richard F Betzel and Danielle S Bassett. Generative models for network neuroscience: prospects and promise. *J. R. Soc. Interface*, 14(136):20170623, 2017.

[41] C. J. Stam and E. C W van Straaten. The organization of physiological brain networks. *Clin. Neurophysiol.*, 123(6):

1067–1087, 2012. ISSN 13882457.

[42] Claire Ribrault, Ken Sekimoto, and Antoine Triller. From the stochasticity of molecular processes to the variability of synaptic transmission. *Nat. Rev. Neurosci.*, 12(7):375–387, 2011.

[43] Gaëlle Doucet, Mikaël Naveau, Laurent Petit, Nicolas Delcroix, Laure Zago, Fabrice Crivello, Gaël Jobard, Nathalie Tzourio-Mazoyer, Bernard Mazoyer, Emmanuel Mellet, and Marc Joliot. Brain activity at rest: a multiscale hierarchical functional organization. *J. Neurophysiol.*, 105(6):2753–2763, 2011. ISSN 1522-1598.

[44] Marcus Kaiser and Claus C Hilgetag. Nonoptimal component placement, but short processing paths, due to long-distance projections in neural systems. *PLoS Comput. Biol.*, 2(7):e95, 2006.

[45] N. T. Markov et al. A weighted and directed interareal connectivity matrix for macaque cerebral cortex. *Cereb. Cortex*, 24(1):17–36, 2014.

[46] Mária Ercsey-Ravasz, Nikola T. Markov, Camille Lamy, David C. VanEssen, Kenneth Knoblauch, Zoltán Toroczkai, and Henry Kennedy. A Predictive Network Model of Cerebral Cortical Connectivity Based on a Distance Rule. *Neuron*, 80(1):184–197, 2013.